CARBON FIBERS DERIVED FROM MESOPHASE PITCH: EFFECT OF AXIAL CRYSTALLITE SIZE AND PROPERTIES

Victor Bermudez, Amod A. Ogale

Department of Chemical and Biomolecular Engineering and Center for Advanced Engineering Fibers and Films (CAEFF)

Clemson, South Carolina

ABSTRACT

Mesophase pitch (MP) offers an interesting potential as an inexpensive precursor of carbon fibers with remarkable axial modulus and electrical and thermal conductivities. Their tensile and compressive strength must be improved before use in structural applications is technically feasible. With that aim, the present work investigates the relationship between axial crystallite size and properties resulting from different drawdown ratios (DDRs) during melt spinning. A synthetic, naphthalene-based ARMP was spun through ultrafine-diameter spinnerets into precursor fibers, which were converted to carbon fibers following stabilization and high temperature treatment at 2100 °C. Raman spectroscopy of the carbon fibers revealed a negative correlation between crystallite size along the fiber axis and DDR, while scanning electron microscopy of their longitudinal surface revealed an increasing fibril thickness with decreasing DDR, which has not been reported in prior literature studies. Ongoing work will investigate the effect of these microstructural features on mechanical properties of carbon fibers.

SAMPE Conference Proceedings. Charlotte, NC, May 20-23, 2019. Society for the Advancement of Material and Process Engineering – North America.

1. INTRODUCTION

Carbon fibers (CFs) from mesophase pitch (MP) precursor exhibit the highest tensile modulus and electrical/thermal conductivities among all types of carbon fibers, due to their highly graphitic microstructure. With values exceeding 500 GPa and 200 W/m·K for tensile modulus and axial thermal conductivity, and small negative values for coefficient of thermal expansion (CTE), mesophase pitch-based carbon fibers (MPCFs) are preferred to CFs derived from polyacrylonitrile (PAN), rayon or lignin in applications in which dimensional stability and thermal dissipation are critical [1]. Aerospace engine nozzles and brake discs, electromagnetic interference shielding, heat sinks and low thermal expansion solders are some examples of such applications [1-4]. However, mechanical strength of MPCFs is inferior to that of PAN-based CFs, the later reaching up to 6 GPa of tensile strength compared to up to 3 GPa for the former [5]. Compressive strength follows the same behavior (~ 0.7 GPa for the stiffest MPCFs vs. ~ 2 GPa for PAN-base CFs). Therefore, use of carbon fiber reinforced composites in structural applications, including medium to large-scale use in aerospace and automotive, is exclusive to PAN-based CFs [6], which have a 90 % share of the worldwide carbon fiber market [5].

In spite of their present mechanical strength-related limitations, research on MPCFs is justified by the potential of MP as low-cost precursor for high performance carbon fibers (HPCFs), since it can be obtained from inexpensive residues of petroleum and coal tar refining and it can give a carbon yield of about 75 % as compared to only ~ 45 % from PAN [7]. In addition, the production of PAN and the oxidative stabilization and carbonization of PAN-based CFs release toxic gases such as HCN, while the heat treatment of pitch produces primarily CO_2 [8]. The challenge for MPCFs remains on improving their strength and at the same time maintaining their superior modulus and electrical/thermal conductivities.

MPCF processing involves three main steps, namely (i) melt-spinning where fiber is formed, (ii) thermosetting where the fiber is rendered infusible, and (iii) carbonization where carbon is concentrated and crystallinity is developed. The present study focuses on the fiber formation step in its approach to enhance MPCF strength. While previous studies have explored other steps of MPCF processing with the same aim of improving strength of MPCFs, such as thermosetting and carbonization [9,10], we believe that emphasis on melt-spinning conditions is a more fundamental methodology because it is during this step that fiber microstructure develops, which largely determines the properties of the resulting CFs [11].

Melt-spinning involves three main steps, namely melting, extrusion and drawing. It is this last step that the present study will focus on, because it is the less studied of the three. For MPCFs, the majority of experimental studies on melt spinning have investigated variables in the melting and extrusion steps [11-15]. However, the effect of drawdown on the properties of resulting MPCFs have not been systematically investigated. While the relationship between drawing and fiber properties has been extensively reported for polymer and PAN fibers, establishing that the tensile properties of carbon fibers improve with increasing drawdown ratio during PAN fiber formation [16,17], those results cannot be extrapolated to MPCFs because mesophase pitch is a liquid crystal consisting of disc-like molecules a few nanometers long, different to extended, long-chain PAN molecules (about 100 nm long) [7]. Therefore, the goal of the present study is to evaluate the effect of drawdown ratio (DDR) on the microstructure and properties of mesophase pitch-based carbon fibers.

2. EXPERIMENTATION

2.1 Materials

ARMP mesophase pitch was used as precursor material for the processing of precursor fibers. This synthetic, naphthalene-based pitch with 100 % mesophase content is produced by Mitsubishi Gas Chemical Corporation and has a measured softening point of 281 ± 17 °C (ASTM D3104 standard procedure in a Mettler Toledo FP90 with a heating rate of 10 °C/min).

2.2 Processing of fibers

Melt spinning of the powdered, degasified ARMP pitch was performed in a batch unit operating at constant volumetric flow rate. The spinning temperature was set at 300 °C. Four custom-designed spinnerets were used, each one with a specific set of ultrafine capillary diameter, capillary length and number of holes: i) 50 μm, 250 μm and 18 holes; ii) 75 μm, 370 μm and 18 holes; iii) 100 μm, 200 μm and 12 holes; and iv) 150 μm, 300 μm and 12 holes. This choice of spinnerets allowed for the spinning of fibers of comparable diameters with contrasting drawdown ratios, and for the extrusion from the finest capillary diameters with moderate shear rates. Extruded fibers were drawn by a roll spinning at speeds in the range 25-700 m/min, and solidified by natural air convection.

As-spun fibers obtained by the procedure above were oxidatively stabilized in a forced convection oven set to 220-240 °C for a period of time in the range 30-75 hours, to achieve a 12 % weight gain. Oxidized, infusible fibers were graphitized at 2100 °C with a heating ramp of 8 °C/min, using a high temperature furnace (HP50, Astro 1000 or Astro 1100, Thermal Technology LLC) under

helium atmosphere. The final temperature was held for 30 minutes, after which the furnace was cooled down to room temperature at a controlled rate.

2.3 Characterization of fibers

As-spun fiber diameter, d_L, and carbon fiber diameter, d_{cf}, was measured by laser diffraction. DDR was calculated from the as-spun fiber diameter and the spinneret capillary diameter, d_0, according to equation 1:

$$DDR=(d_0/d_L)^2 \quad (1)$$

Longitudinal textures of carbon fibers were examined by scanning electron microscopy (SEM) of the exposed cross-sections, using a Hitachi S4800 at accelerating voltages in the range 3.0-15.0 kV. The longitudinal surface was observed by cutting fiber samples to ~ 15 mm length and placing them perpendicularly to the electron beam.

Axial size and degree of perfection of carbon fiber crystallites were quantified as crystallite length, L_a, and distance between point-like defects, L_D, by Raman spectroscopy, using a Renishaw Ramascope spectrometer with a laser power and wavelength of 25 mW and 785 nm. Raman spectra were curve-fitted using Wire 3.4 to determine area ratio (A_D/A_G) of the characteristic carbon bands **D** and **G**, and the respective Cançado et al correlation [18] was used to estimate L_a, equation 2:

$$L_a = (2.4 \times 10^{-10})\lambda_l^4(A_D/A_G)^{-1} \quad (2)$$

Electrical resistivity of single CF filaments was determined by a two-probe method with a gage length of 10 mm. The Lavin et al. correlation [19] was used to estimate the thermal conductivity

from electrical resistivity measurements. Values of measured electrical resistivity and correlated thermal conductivity are reported as average with a 95 % level of confidence from a t-statistic.

3. RESULTS

3.1 Melt spinning

Eight precursor fiber samples were obtained and named A through H, with the following DDRs: A, 209 ± 18; B, 17 ± 3; C, 58 ± 10; D, 32 ± 3; E, 44 ± 5; F, 19 ± 3; G, 189 ± 29; H, 14 ± 2.

3.2 Scanning electron microscopy

Figure 1 shows the SEM micrographs of longitudinal surfaces of representative specimens from CF samples. Samples are paired according to equivalent carbon fiber diameter, as follows: A and B, ~ 12 μm; C and D, ~11 μm; E and F, ~ 9 μm; and G and H, ~ 8 μm. All samples exhibit definite fibrils running parallel to the fiber axis, as described in previous works on MPCFs [20,21]. However, the samples of low DDR of each pair present thicker fibrils with clearer contours than those of their high-DDR counterparts, which is an indication of favored growth of carbon planes during carbonization. The average thickness of fibrils for samples of high DDR was measured in the range 69-103 nm, while that for samples of low DDR was measured in the range 158-220 nm. The widening of fibrils with increasing HTT has been previously reported by Korai et al., who measured a fibril thickness of 100 nm for MPCFs heat-treated to 1500 °C [21]. However, this is

the first time textural development has been systematically reported as a function of DDR used during pitch fiber spinning.

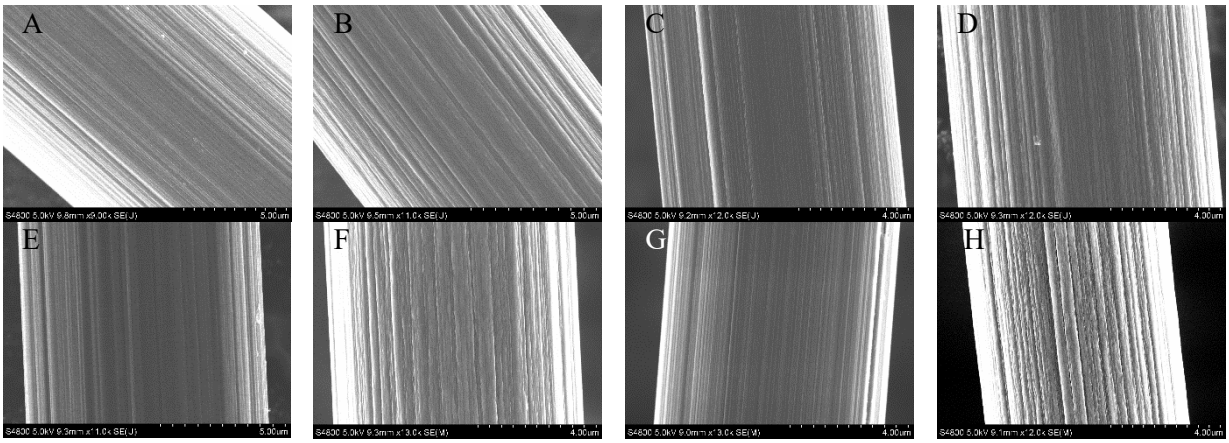

Figure 1. SEM of longitudinal surface of CFs heat-treated to 2100 °C. Average measured fibril thickness of each sample as follows (nm): A, 102 ± 8; B, 220 ± 6; C, 79 ± 3; D, 172 ± 8; E, 103 ± 3; F, 158 ± 9; G, 69 ± 5; H, 181 ± 8

3.3 Raman spectroscopy

Figure 2 shows Raman spectra of samples A through H arranged in pairs. All spectra show the **D** and **G** bands characteristic of carbon materials, at around 1350 and 1580 cm^{-1}, respectively. Bands **D'** and **G'** also appear, at around 1620 and 2650 cm^{-1} [18]. For pairs C-D, E-F and G-H, the sample with smaller DDR has the more intense **G** band, which is representative of graphitic ordering [7]. Therefore, for those pairs, the sample with smaller DDR has the smaller A_D/A_G, which translates into a larger crystallite length according to equation 2. Estimated values of L_a are as follows, in nm: A, 75 ± 2; B, 71 ± 1; C, 65 ± 2; D, 73 ± 1; E, 71 ± 1; F, 75 ± 1; G, 58 ± 1; H, 85 ± 2. In other words, the samples with smaller DDR in all pairs have bigger crystallites.

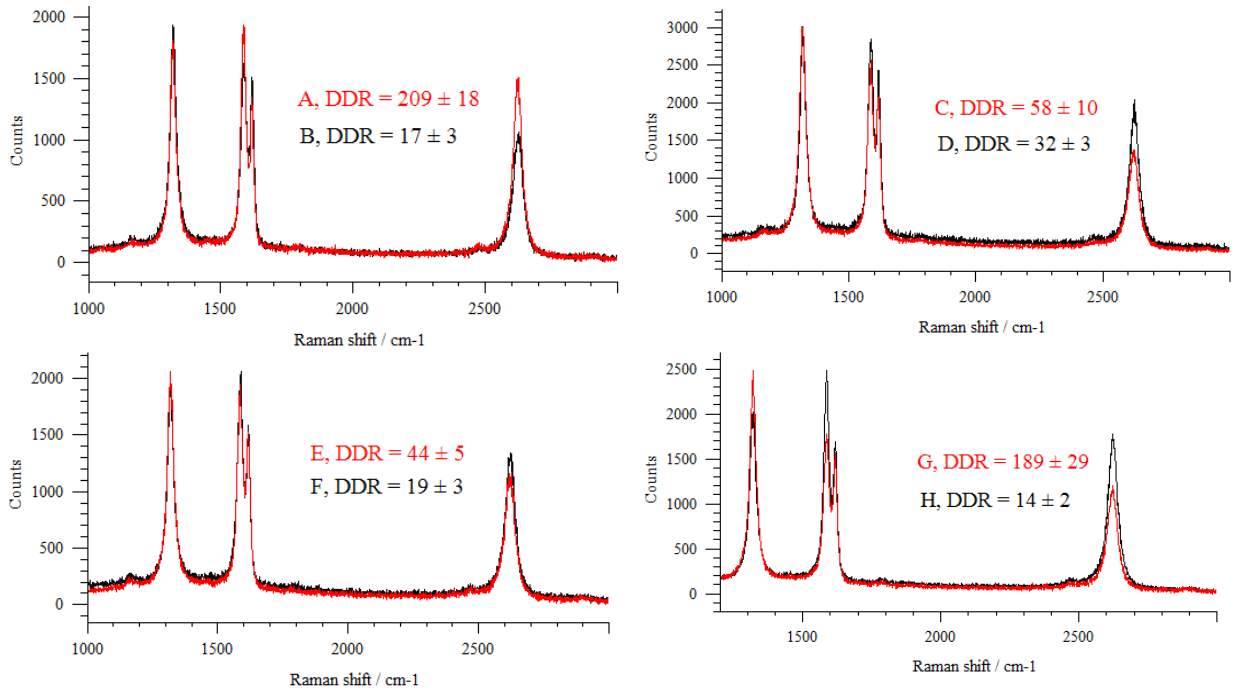

Figure 2. Raman spectra of CF samples. A_D/A_G of samples is as follows: A, 1.21; B, 1.29; C, 1.40; D, 1.25; E, 1.28; F, 1.21; G, 1.58; H, 1.07

Average L_a across samples was ~ 72 nm. K1100 CFs were used as a control sample and displayed $L_a = 160 \pm 5$ nm; for reference, L_a measured by x-ray diffraction has been reported around 120 nm for K1100 CFs [22].

For pairs C-D, E-F and G-H, the sample with smaller DDR has the more intense **G'** band. Previous studies have reported that the intensity **G'** band decreases with increasing numbers of graphene layers [23], therefore it could be expected that the samples with smaller DDR have a smaller crystallite stacking height.

3.4 Thermal conductivity

Correlated thermal conductivity of samples A through H was calculated as follows: A, 258 ± 32; B, 188 ± 11; C, 168 ± 26; D, 186 ± 13; E, 215 ± 30; F, 213 ± 13, G, 209 ± 5; H, 260 ± 62. For pairs C-D and G-H, smaller DDR results in higher electrical conductivity, while the opposite is true for pairs A-B and E-F; however, only for pair A-B is the difference significant. The thermal conductivity ranged from 168 to 260 W/m·K, averaging 213 W/m·K. These values are lower than those from previous studies on CFs based on AR-type MPs, with some authors reporting an correlated thermal conductivity of ~ 550 W/m·K for CFs heat-treated to 2600 °C [22]. K1100 CFs were used as a control sample with correlated $\kappa = 857 \pm 83$ W/m·K; such value is consistent with the one reported in the literature [5].

4. CONCLUSIONS

Carbon fibers were obtained from a AR-grade mesophase pitch using a set of spinnerets with capillary diameters in the range 50-150 μm, and a moderately high graphitization temperature of 2100 °C. The results of this study have found novel visual evidence for the effect of DDR on the surface longitudinal microstructure, with decreasing DDR leading to thicker fibrils along the fiber axis. Evidence for a negative effect of DDR on crystallite size has also been provided. Future work will focus on the effects of the microstructural features on the mechanical strength and transport properties of carbon fibers.

5. REFERENCES

[1] Huson M. High-performance pitch-based carbon fibers. In: Anonymous Structure and Properties of High-Performance Fibers: Elsevier; 2017, p. 31-78.

[2] Luo R, Liu T, Li J, Zhang H, Chen Z, Tian G. Thermophysical properties of carbon/carbon composites and physical mechanism of thermal expansion and thermal conductivity. Carbon 2004;42:2887-95.

[3] Chung DDL. Composite Materials. Kirkâ€□Othmer Encyclopedia of Chemical Technology 2004.

[4] Morgan P. Carbon Fibers and Their Composites. Boca Raton, FL: CRC Press, 2005.

[5] Jeon Y, Alway-Cooper R, Morales M, Ogale AA. Chapter 2.8 - Carbon Fibers. In: Somiya S, editor. Handbook of Advanced Ceramics (Second Edition), Oxford: Academic Press; 2013, p. 143-154.

[6] Newcomb BA. Processing, structure, and properties of carbon fibers. Composites Part A: Applied Science and Manufacturing 2016;91:262-82.

[7] Frank E, Steudle LM, Ingildeev D, Spoerl JM, Buchmeiser MR. Carbon fibers: precursor systems, processing, structure, and properties. Angewandte Chemie International Edition 2014;53:5262-98.

[8] Park S, Heo G. Precursors and Manufacturing of Carbon Fibers. In: Park S, editor. Carbon Fibers, Dordrecht: Springer Netherlands; 2015, p. 31-66.

[9] Park M, Jung M, Lee Y. Significant reduction in stabilization temperature and improved mechanical/electrical properties of pitch-based carbon fibers by electron beam irradiation. Journal of Industrial and Engineering Chemistry 2016;37:277-87.

[10] Greene M, Schwartz RW, Treleaven J. Short residence time graphitization of mesophase pitch-based carbon fibers. Carbon 2002;40:1217-26.

[11] Edie D. The effect of processing on the structure and properties of carbon fibers. Carbon 1998;36:345-62.

[12] Ōtani S, Ōya A. Progress of Pitch-Based Carbon Fiber in Japan. In: Anonymous Petroleum-Derived Carbons: American Chemical Society; 1986, p. 323-334.

[13] Hamada T, Nishida T, Sajiki Y, Matsumoto M, Endo M. Structures and physical properties of carbon fibers from coal tar mesophase pitch. J Mater Res 1987;2:850-7.

[14] Kundu S, Ogale AA. Rheostructural studies on a synthetic mesophase pitch during transient shear flow. Carbon 2006;44:2224-35.

[15] Matsumoto M, Iwashita T, Arai Y, Tomioka T. Effect of spinning conditions on structures of pitch-based carbon fiber. Carbon 1993;31:715-20.

[16] Wang Y, Wang C, Bai Y, Bo Z. Effect of the drawing process on the wet spinning of polyacrylonitrile fibers in a system of dimethyl sulfoxide and water. J Appl Polym Sci 2007;104:1026-37.

[17] Kirsten M, Meinl J, Schönfeld K, Michaelis A, Cherif C. Characteristics of wet-spun and thermally treated poly acrylonitrile fibers. J Appl Polym Sci 2016;133:43698.

[18] Cançado L, Takai K, Enoki T, Endo M, Kim Y, Mizusaki H et al. General equation for the determination of the crystallite size L a of nanographite by Raman spectroscopy. Appl Phys Lett 2006;88:163106.

[19] Lavin J, Boyington D, Lahijani J, Nysten B, Issi J. The Correlation of Thermal-conductivity With Electrical-resistivity in Mesophase Pitch-based Carbon-fiber. Carbon 1993;31:1001-2.

[20] Yoon S, Korai Y, Mochia I, Yokogawa K, Fukuyama S, Yoshimura M. Axial nano-scale microstructures in graphitized fibers inherited from liquid crystal mesophase pitch. Carbon 1996;34:83-8.

[21] Korai Y, Hong S, Mochida I. Development of longitudinal mesoscopic textures in mesophase pitch-based carbon fibers through heat treatment. Carbon 1999;37:203-11.

[22] Alway-Cooper RM, Anderson DP, Ogale AA. Carbon black modification of mesophase pitch-based carbon fibers. Carbon 2013;59:40-8.

[23] Park JS, Reina A, Saito R, Kong J, Dresselhaus G, Dresselhaus MS. G′ band Raman spectra of single, double and triple layer graphene. Carbon 2009;47:1303-10.